

THE STUDY OF INDICATRICES OF SPACE OBJECT COATINGS IN A CONTROLLED LABORATORY ENVIRONMENT

Koshkin N., Burlak N., Petrov M., Strakhova S.

Astronomical observatory of Odessa university, Odessa, Ukraine
nikkoshkin@onu.edu.ua

ABSTRACT. The indicatrices of light scattering by radiation balance coatings used on space objects (SO) were determined in the laboratory experiment in a controlled condition. The laboratory device for the physical simulation of photometric observations of space objects in orbit, which was used in this case to study optical properties of coating samples, is described. The features of light reflection off plane coating samples, including multi-layer insulation (MLI) blankets, metal surfaces coated with several layers of enamel EP-140, special polyacrylate enamel AK-512 and matte finish Tp-CO-2, were determined. The indicated coatings are compound reflectors which exhibit both diffuse and specular reflections. The data obtained are to be used in the development of computer optical-geometric models of space objects or their fragments (space debris) to interpret the photometry results for real space objects.

1. Introduction

The optical-geometric modelling of a target object and its observing conditions is applied to test of methods for obtaining information on the properties and behaviour of space objects in orbit using photometric observations. To that end, both computer (Melikyants, 2007; Willison & Bédard, 2015), and physical (Koshkin, 1989) simulations have been used in the Department of Space Research of the Astronomical Observatory of Odessa University.

Proper simulation supposes knowledge of optical properties of space object surfaces, namely light-scattering indicatrices and spectral reflectance. Ideal (either theoretical or empirical) functions for light scattering from uniform surfaces (Fairbairn, 2005) are often used to simplify the problem. However, when sensing man-made objects and surfaces, such ideal functions are hardly feasible and provide results which are inconsistent with observations (Früh & Schildknecht, 2012).

The spectral scattering function or its approximation in either numerical or analytical form should be factored in the computer simulation model (Kanzler, 2015). The geometric conditions of lighting and photometry similar to those for the real objects should be adhered to in case of physical simulation in a controlled laboratory environment with space object models (Koshkin, 1985). It means that when conducting measurements in the laboratory, the conditions of integrated photometric measurements of the space object model as a point-like object should be abided; the model illumination should be provided by a source of light generating the spectral intensity

distribution in the visible spectrum close to the solar one (for colorimetric measurements) with the light beam divergence of about 30'.

The kinematic design of the simulation device should provide the required motion of the model relative to the observer and light source (including the model's spatial orientation and compound rotation around given axes), as well as simulation of simultaneous change of the phase angle, etc.

Scale similarity between the model and target space object, correspondence of coatings' optical properties and simulation of the space object spatial motion ensure conformity between the model photometry and actual observations of the space object.

The aim of this study is to exploit kinematic and photometric capabilities of the laboratory device to measure indicatrices of several real coatings used to radiation balance of space objects. Then, the data obtained can be used in the development of relevant optical-geometric models of space objects or their fragments (space debris).

2. The device for simulation in a controlled laboratory environment

The manufactured device for simulation of the space object photometric observations and measurements of sample indicatrices in a controlled laboratory environment contains three component units: the unit for model (sample') placing and rotation, illumination assembly and photometer.

The model illumination assembly. In terms of design, the model illumination assembly is a collimating system. An aperture of diameter D , which is overlapped by frosted glass and backside illuminated by a high-intensity halogen lamp KGM-12-40 with heat-reflection filter, is placed in the focal plane of the collimating lens. The required light beam divergence of about 30', which simulates the divergence of solar flux, is achieved with the relevant ratio between the diameter of "illuminated" aperture and collimator focus length F .

The photometer unit. The photometer unit is designed for the measurement of the luminous flux from the model as a point-like object. In terms of design, it is achieved by using a long-focus integrating lens with a diameter which exceeds the model size, and thus, is capable to trap all parallel light rays passing from the model towards the photometer. There is a pinhole aperture with the diameter $d = 1$ mm in the focal plane of the lens, which cuts off all

rays from the model at angles exceeding .050. The Fabry lens is attached behind the aperture; it creates an image of the aperture illuminated with the light from the model on the photocathode of light detector – in our case photomultiplier tube FEU-136. The photometer is provided to mount a filter wheel containing three band-pass filters which enable to determine the model's colours in three spectral regions, namely blue, green and red, close to TV-color system.

The mounting of model (sample) placing and rotation.

This assembly comprises an annular guide to mount the small-type stepper motor on whose axis is fixed the model – that ensures proper spatial orientation of the rotation axis. The rotation axis of the observed sample or model keeps its position with respect to the light source and can rotate along with that source relative to the photometer. In the course of all motions and rotations the sample is always kept in the centre of the light beam from the light source and within the photometer field of view.

The whole device was assembled and exploited in the blacked out room. Auxiliary mechanical parts which get into the photometer field of view or the flux from the light source at some conditions, were blackened with black matte finish to eliminate glares and stray extraneous light spots.

3. The study of light-scattering indicatrix of different SO coatings

Different types of coatings are used to maintain proper thermal balance inside of a space craft when it moves outside the Earth's atmosphere, namely multi-layer insulation (MLI) blankets, enamels with various light-scattering properties, metal surfaces, etc. Moreover, spacecrafts usually equipped with solar arrays with photoelectric transducers covered with protective coatings of fused silica, other optical assemblies and components.

Coatings used in the space have different reflectance properties in the visible wavelength range depending on the coating material and its surface microstructure. In general, to describe the reflectance profile for a given surface, it is suggested to use the spectral bidirectional reflectance distribution function (sBRDF) f_r (Willison & Bédard, 2015), which is determined from formula:

$$f_r(\theta_i, \phi_i; \theta_r, \phi_r; \lambda) = \frac{dL_r(E_i; \theta_i, \phi_i; \theta_r, \phi_r; \lambda)}{L_i(\theta_i, \phi_i; \lambda) \cdot \cos \theta_i \cdot d\omega_i} \quad [\text{sr}^{-1}]$$

where L_i and L_r are incident and reflected luminous flux, respectively, and other notations can be understood from Figure 1. It should be noted that sBRDF does not depend on the surface area.

Specific character of the LEO observations is related to their motion with respect to an observer and their rotation around the centre of mass. These factors cause changes in the solar illumination angle, as well as in the angle at which the object is visible to the observer. Therefore, it is suitable to use as a representation of spatial indicatrices a set of expressions of the correlation between the coating sample brightness (in the broadband system) and the angle of its rotation α relative to the phase-angle bisector, at the fixed values of the latter. In this case, all measurements are performed in one and the same plane, that is: $\varphi_i = 0^\circ$; $\varphi_o = 0^\circ$ or 180° .

The angle α varies within the range of $\pm(\pi/2 - \beta/2)$ (see Fig. 1,b).

Using the laboratory simulation device we carried out the study of multi-layer coatings consisting of the atmosphere-resistant epoxy enamels EP-140, special polyacrylate enamels AK-512 and matte finish coatings Tp-CO-2 (Simulation, 1971; Ivanov, 1969), as well as MLI blankets covered externally of white glass fabric.

The brightness of the illuminated coating sample in the linear (or logarithmic) scale in relative units is shown along the Y-axis in the below-presented images of the spatial indicatrix sections. The brightness was determined by measuring the intensity of the reflected luminous flux and its normalisation to account for the geometric factors. The X-axis shows the angle of the sample's rotation in the phase-angle plane determined as the angle between the normal to the mean plane of the sample's surface and the phase-angle bisector.

The measurements were conducted at three different phase angles within the range of 45° - 135° . The speciality of such measurement and representation of indicatrices is that the start point of the plotted curve corresponds to grazing incidence of the light beam onto the sample therefore several first points of the curve correspond to the

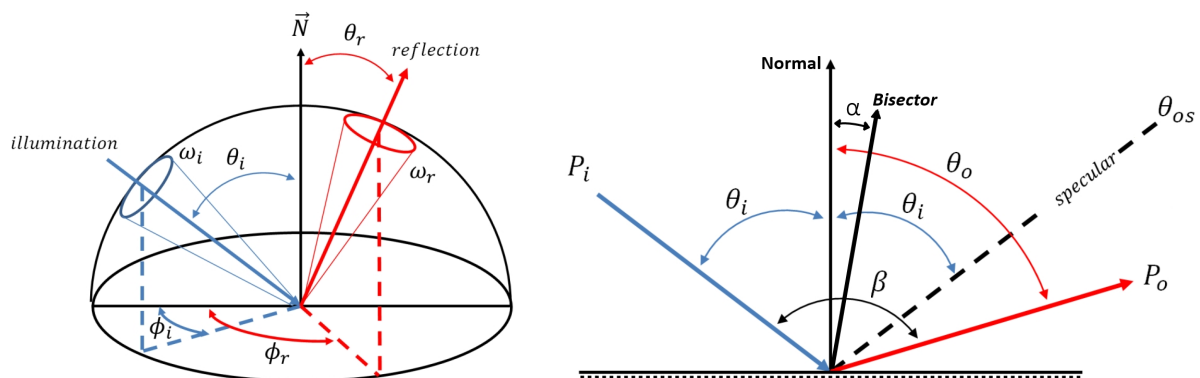


Figure 1: a) The spatial geometry of the light scattering from surface piece (adopted from Willison, 2015); b) The geometry of indicatrix measurements in the phase-angle plane; the β is phase angle.

interval when operation lighting conditions for that sample are achieved, and the indicatrix in this segment can be inconsistent with the actual brightness of the coating. The ending points of the curve must correspond to the observation of the sample surface at the angles close to 90° , and division by the relevant reflection angle cosine results in wider spread of points in this segment of the graph.

D1 – Material: Alloy AMg6M. Coating: primer AK-070 (1) Industry Standard (OST) 6-10-401-76. Enamel EP-140, white (2) Specifications (TU) 6-10-599-74. Enamel AK-512, white (2) State Industry Standard (GOST) 23171-78 and VD 23171-78.

Let us proceed to the discussion of the obtained indicatrices of light-scattering by coating samples. Fig. 2 shows the brightness indicatrices of the plane sample D1 coated with the primer AK-070 (one layer), enamel EP-140 of white colour (two layers) and enamel AK-512 of white colour (two layers). This coating is a compound reflector of light which exhibits both diffuse and specular reflections. At small phase angles ($\leq 45^\circ$), the inner diffuse reflection prevails over the brightness of specular reflection off the external layer. The diffuse reflection indicatrix is just slightly deformed comparing to the ideal Lambert's indicatrix for which the brightness does not depend on the angle at which the coating sample surface is observed (Ivanov, 1969). With the increased phase angle the specular reflection brightness increases rapidly, and at $\Phi=120^\circ$ it is 10-100 times higher than the diffuse reflection brightness.

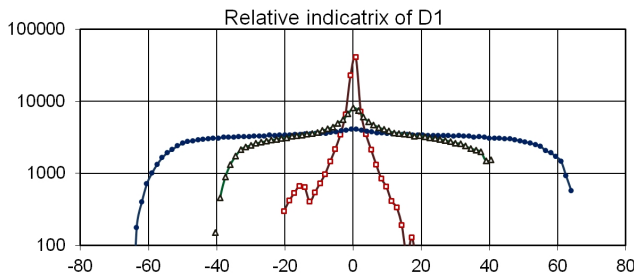


Figure 2: Brightness indicatrix of flat sample D1 for different phase angles: full circles – $\beta=45^\circ$, open triangles – $\beta=90^\circ$, open squares – $\beta=135^\circ$.

Apart from the discussed ones, the indicatrices of the same coating were obtained with different orientation of the phase-angle plane relative to the sample (the phase-angle plane is rotated by 90° with respect to the normal to the sample). The characteristics of these curves have not changed comparing to the data presented in Fig. 2, which were obtained at the same phase angles.

It is necessary to pay attention to the behaviour of spectral content of the light reflected off the coating sample D1. We conducted preliminary measurements of the three-colour reflectance for this and other samples at different phase angles. At that, a noticeable redshift of the light reflected by the coating sample D1 at the instants of specular component appearance can be marked out. The degree of this redshift increases with the increasing phase angle.

D2 – Material: Alloy AMg6M. Coating: Enamel AK-512, white (2) State Industry Standard (GOST) 23171-78. Matte finish Tp-CO-2 (2) Industry Standard (OST) 92-1000-76.

The plane surface of the second coating sample labelled in our study as D2 is coated with two layers of enamel AK-512 and two layers of white matte finish Tp-CO-2. The indicatrices of light-scattering by this coating sample are shown in Fig. 3. In contrast to the above, this coating sample only exhibits the diffuse reflection component in the studied range of phase angles with the reflection indicatrix close to the Lambert one. A perceptible specular component appears at the phase angles $\geq 160^\circ$ while the indicatrix which is just slightly elongated in the direction of the specular reflection can be observed at smaller phase angles (120° - 140°).

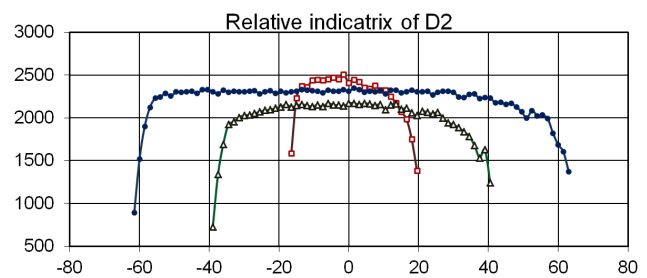


Figure 3: Brightness indicatrix of flat sample D2 for different phase angles: full circles – $\beta=45^\circ$, open triangles – $\beta=90^\circ$, open squares – $\beta=135^\circ$.

The light-scattering indicatrices of the plane sample of the MLI exterior coating which is made of white glass fabric, is presented in Fig. 4.

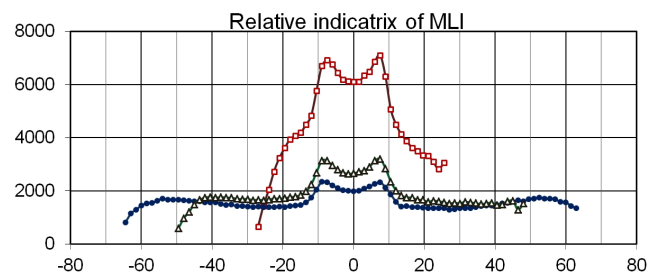


Figure 4: Brightness indicatrix of flat sample MLI for different phase angles: full circles – $\beta=45^\circ$, open triangles – $\beta=75^\circ$, open squares – $\beta=120^\circ$.

The cell structure of this coating sample, as well as its high transparency (transmission up to 40% of the solar radiation), results in complex behaviour of its brightness with changing lighting and observation conditions. Its indicatrix exhibits several brightness peaks, the highest two of them, i.e. the pre- and post-specular reflections, which are symmetric with respect to the specular reflection from the coating sample surface. Moreover, the local brightness maximums are observed when either the angle of light incidence or the angle of observation is approaching to the grazing one; at that, the maximum brightness values and their extent increase with decreasing phase angle; meanwhile, such maximums are not observed

at $\Phi > 90^\circ$. The study of indicatrices of glass fabric samples with the substrate of light-absorbing material or corrugated aluminium foil showed their identity, though the total brightness was slightly higher for the second sample. However, the presence of two accentuated directions on the glass fabric surface due to the material filament flow also results in the dependence of the spatial scattering indicatrix on the position of the phase-angle plane relative to those marked out directions.

Fig. 5 shows the indicatrices of the MLI coating sample when the phase-angle plane makes an angle of 45° with the glass fabric filament flow. In this case, the double brightness peak (corresponding to the pre- and post-specular reflections) is significantly broadened, and the brightness increase at large angles of light incidence and reflection is no longer observed. It should be noted that the angular distance between the pre- and post-specular peaks does not depend on the phase angle; however, it depends on the orientation of the MLI blanket sample.

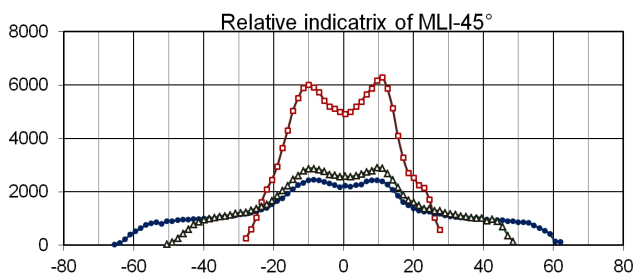


Figure 5: Brightness indicatrix of flat sample MLI for different phase angles: full circles – $\beta=45^\circ$, open triangles – $\beta=75^\circ$, open squares – $\beta=120^\circ$.

Space object surface-integrated indicatrix of this coating sample with the surface imperfections was also investigated (such ‘quilted’ MLI blanket is apparently tufted across, and there is some curvature, as well as structural elements on the space object surface). The indicatrices of the MLI blanket sample with soft plane base tufted in the square lattice points with stitch spacing of ~ 5 mm and the depth of local imperfections of ~ 0.5 mm, which cause a significant surface curvature of sample (MLI-G-15), are also investigated. It should be noted that at the phase angles of 40° – 60° the surface-integrated indicatrix appears smoothed with just a subtle elongation in the direction of the specular reflection from the mean surface. At the phase angles $\geq 90^\circ$ this brightness peak tends to double due to the glass fabric structure. With the lower ratio between the stitch depth and spacing, i.e. with the relatively smaller scale of imperfections on the MLI coating, the indicatrix takes the form which is typical for the plane coating sample. It is evident that any imperfections on the space object surface can not significantly change the integrated indicatrix of the MLI coating.

In addition to the above-described coating samples, the solar array cell indicatrix was also measured. Due to the smooth polished dielectric surface of the solar cell coating, the indicatrix has the form of the δ function; and the linear dynamic range of the photometric equipment is not sufficient to measure the drop in brightness when

either diffuse or specular reflection off this coating sample occurs. However, as is known, the solar arrays consist of many thousands of solar cells, and because of parallel misalignment of their surfaces the integrated indicatrix will not be close to the δ function due to large deviations in averaging of individual indicatrices; moreover, there are such design features as parallel misalignment of the solar panel sections and their flexure; therefore, when modelling photometric characteristics of the solar array working plane, it is only the similarity of the indicatrix integrated parameters that should be sought.

4. Conclusions

To ensure the photometric, as well as geometric, equivalence of models (physical and mathematical ones) and real space objects, it is essential to use coatings identical in their optical properties. Moreover, it is necessary to aim at correct simulation just of those surface-integrated photometric characteristics of large components and object integrally. To that end, we carried out the measurement of optical properties of a set of original coatings, in particular, their light-scattering indicatrices in the visible spectrum. The indicatrix of light scattering from the surface is essential in the integrated photometry (in the visible wavelength range) as an instrument of optical remote sensing, because it specifies the spatial structure of light-scattering field, and thus, the appearance of the light curve expressing the brightness change with time, which provides information on the physical properties of the object itself.

References

- Bédard D., Lévesque M., Wallace B.: 2011, in *Proc. of AMOS Conf.*
- Bédard D., Wade Gregg A.: 2014, in *Proc. of AMOS Conf.*
- Früh C., Schildknecht Th.: 2012, 63-rd International Astronautical Congress, Naples, Italy, IAC-12-A6.2.6.
- Fairbairn M.B.: 2005, *J. of the Roy. Astron. Soc. of Canada*, **99**, No. 3, p.92 (2005JRASC..99...92F).
- Ivanov A.P.: 1969, *Optics of scattering media. Nauka i Technika*, 592.
- Kanzler R. et al.: 2015, in *Proc. of AMOS Conf.*
- Koshkin N.: 1985, The laboratory device for simulating the observations of space objects. Certificate of authorship UdSSR No. 229507 – 1985.
- Koshkin N.I.: 1989, *Astronomicheskij Vestnik* (Moscow, USSR), **22**, No. 2, 159 (1989RpScT...2...13K). (English: JPRS Report: Science and Technology. USSR: Space p.13 (SEE N89-29354 24-12))
- Melikyants S., Shakun L. et al.: 2007, *Odessa Astron. Publ.*, **20**, 72 (2007OAP...20...72M).
- Simulation of thermal conditions of the spacecraft and its environment /Eds. G.Petrov and M.Kroshkin, Mashinostroenie, 1971, P. 382.
- Willison A., Bédard D.: 2015, in *Proc. of AMOS Conf.*